ORIGINAL CONTRIBUTION

Template synthesis of tin-doped indium oxide (ITO)/polymer and the corresponding carbon composite hollow colloids

Huifang Xu · Shujiang Ding · Wei Wei ·
Chengliang Zhang · Xiaozhong Qu · Jiguang Liu ·
Zhenzhong Yang

Abstract SnO_2, In_2O_3, and Sn-doped In_2O_3 (ITO)/polymer and the corresponding carbon composite hollow colloids are template synthesized. It is essential that the sulfonated gel shell of the cross-linked polystyrene hollow colloid can favorably induce adsorption of target precursors. After being calcined in air to remove the template, SnO_2, In_2O_3, and ITO hollow colloids are obtained. Because the cross-linked polymer gel can be transformed into carbon in nitrogen at higher temperature such as 800 °C, metal oxide/carbon hollow colloids are consequently derived, whose shells are mesoporous. The SnO_2-, In_2O_3-, and ITO-containing polymer or carbon composite hollow colloids will be promising in sensors, catalysts, and fuel cells as electrode materials.

Keywords Hollow colloid · Polymeric gel · Template synthesis · Metal oxide · Carbon

Introduction

Inorganic oxide/polymer composite hollow colloids have gained extensive interests because of their attractive performances such as low density, high specific surface area, and short transportation pathway through the shell. They are promising in many fields such as light-weight fillers, catalysis, and controllable delivery [1–3]. Tin oxide, indium oxide, and tin-doped indium oxide (ITO) are series of important metal oxides and widely used as optical devices, electrode materials, and sensors because of their tunable electrical conductivity and high transparency at visible light wavelengths [4–11]. Over the past decades, many efforts have been made to fabricate their thin films, nanoparticles, nanowires, nanorods, and hollow spheres such as electron-beam deposition, chemical vapor deposition, laser ablation, and sol–gel technology [12–18]. Indium oxide hollow colloids have displayed enhanced performance as photocatalysts than the corresponding bulk counterpart [17]. Tin oxide hollow colloids are considered more suitable as sensor materials than other morphological ones [18]. It is also interesting to support the oxides with carbon to enhance conductivity and stability at high temperature [19, 20]. Tin oxide/carbon composite materials have shown higher specific capacity than commercialized graphite as electrode materials [21, 22]. The synthesis of those hollow colloids usually involves many steps such as core template modification and removal of the template either by dissolution or by calcination. The shell will usually be fractured. Therefore, it is required to develop a facile and general procedure to synthesize ITO/polymer composites and the corresponding carbon hollow colloids.

In this study, we extend polymeric gel-induced favorable growth of functional materials using a sulfonated polystyrene (PS) layer of the hollow colloid templates [23, 24], to synthesize tin oxide, indium oxide, and ITO composite hollow colloids. The corresponding pure SnO_2, In_2O_3, and ITO hollow colloids are achieved by heating the composite colloids in air to remove polymer templates. Carbon/oxide composite hollow colloids are prepared by carbonization of the polymer templates at high temperature in nitrogen.

H. Xu · S. Ding · W. Wei · C. Zhang · X. Qu · J. Liu ·
Z. Yang (✉)
State Key Laboratory of Polymer Physics and Chemistry,
Institute of Chemistry, Chinese Academy of Sciences,
Beijing 100080, China
e-mail: yangzz@iccas.ac.cn

Experimental

Samples synthesis

Sulfonated PS gel colloid templates Colloid gel templates were achieved by sulfonation of the cross-linked PS hollow colloids. The freeze-dried PS colloids were dispersed into a large amount of concentrated sulfuric acid at 40 °C for varied time to control the thickness of the sulfonated PS gel layers. The sulfonated PS gel colloids were washed with water/ethanol. Two representative gel templates S1 and S2 were achieved by sulfonation of the corresponding cross-linked PS hollow colloids about 500 nm in diameter for 1 and 3 h, respectively [23].

SnO_2 and Sn-doped $In(OH)_3$/polymer composite and SnO_2, In_2O_3, and ITO hollow colloids A typical procedure was followed: 50 mg of S2 colloid was dispersed into 2 ml of 1 M $SnCl_4$ aqueous under stirring for 24 h for the salt to be absorbed within the colloid. Afterwards, the above colloids were washed with distilled water twice and then dispersed into 4 ml of distilled water at a temperature 80 °C for 72 h to grow the crystalline SnO_2. $In(OH)_3$ composite hollow colloids were accordingly synthesized by using a $In(NO_3)_3$ solution instead and further reacted at pH ~9 by adding 1 ml of 1 M ammonia aqueous at room temperature for 8 h. In the case of forming ITO composite hollow colloids, a mixture with varied atomic ratio of $In(NO_3)_3$ and $SnCl_4$ was absorbed within S2 colloids and further reacted in 1 ml of 1 M ammonia aqueous at room temperature for 8 h. The as-prepared In–Sn hydroxide/S2 composite hollow colloids were calcined in air at 450 °C for 2 h to obtain ITO hollow colloids.

SnO_2, In_2O_3 and ITO/carbon composite hollow colloids The as-prepared SnO_2, $In(OH)_3$, and Sn-doped $In(OH)_3$/S2 composite hollow colloids were treated up to 800 °C in nitrogen.

Characterization

The colloids were dispersed in ethanol and spread on carbon-coated copper grids for transmission electron microscopy (TEM; JEOL 100CX TEM operating at 100 kV). High resolution TEM (HR-TEM) and selected area electron diffraction analysis (SAED) measurements were performed with HITACHI H-9000NAR electron microscope operated at 300 kV. Scanning electron microscopy (SEM) measurement and energy-dispersive X-ray (EDX) analysis were performed with a HITACHI S-4300 instrument operated at an accelerating voltage of 15 kV. The samples were dried at ambient temperature and vacuum sputtered with Pt about an average size of 3 nm. Wide-angle X-ray powder scattering

(Rigaku D/max-2500) was used to characterize the crystalline phase. Inorganic oxide content of the composite colloids was determined by thermogravimetric analysis (TGA; PerkinElmer analyzer Pyris 1 TGA) in the temperature range of 30–800 °C in nitrogen at a heating rate 10 °C/min. Fourier transform infrared (FT-IR) spectra were recorded using a Bruker Equinox 55 spectrometer with samples pressed into KBr pellets. Nitrogen adsorption was performed on a Micromeritics ASAP 2020M Surface Area and Porosity Analyzer. Raman spectra of the carbon hollow samples were characterized by Bruker Equinox 55 spectrometer.

Results and discussion

Sulfonated PS hollow colloids

Sulfonated PS gel hollow colloids [23] were used to template synthesize the semiconductor composite colloids. The parent polymer hollow colloids are mainly composed of a linear PS shell skeleton. To strengthen the polymer shell, a swelling radical polymerization of styrene/divinylbenzene mixture was carried out within the parent PS shell at 80 °C. A representative cross-linked PS hollow colloid was synthesized at a given monomer weight ratio 1:1 and a weight ratio 1:1 of the monomer mixture to the parent hollow colloid. After being treated with solvents such as dimethylformamide, the spherical contour was preserved. In comparison, the parent hollow colloid was completely dissolved. A series of gel colloids were prepared by sulfonation of the cross-linked PS hollow colloids with concentrated sulfuric acid, whose gel thickness was controlled by sulfonation temperature and time [23]. Two representative gel hollow colloids S1 and S2 were accordingly derived by sulfonation at a given temperature 40 °C for 1 and 3 h, respectively. Both gel colloids are hollow with the spherical contour well preserved (Fig. 1). In comparison, gel colloids derived from linear PS hollow colloids were collapsed to lose the spherical contour after being dried [24], which will cause difficulties for further growth of composite shells. Thus, cross-linked gel hollow colloids were used in our study. The derived sulfonic acid and sulfone groups were detected by FT-IR (Fig. 2). The characteristic band at 1,128 cm^{-1} is related to the sulfone group ($-SO_2-$). The bands at 670, 1,176, and 1,222 cm^{-1} are assigned to the derived sulfonic acid group ($-SO_3H$). The characteristic bands of S2 disappeared after carbonization as discussed as follows (Fig. 2d).

SnO_2, In_2O_3, and ITO hollow colloids

The negatively charged sulfonated gel layer can adsorb metal cations, facilitating a further in situ favorable growth

Fig. 1 SEM and *inset* TEM images of two representative gel hollow colloids with varied sulfonation degree: **a** S1, **b** S2
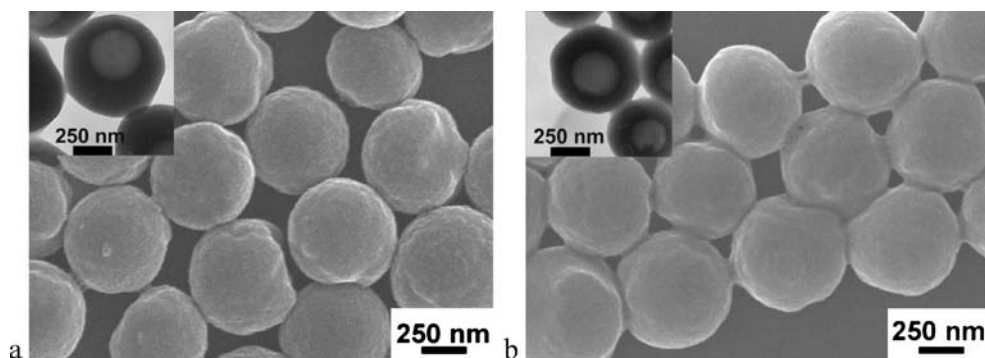
of metal oxides such as SnO_2 and $In(OH)_3$. The S2 colloid was selected as a template to increase the adsorption amount of the precursors. SnO_2/S2 composite hollow colloids were prepared by one-step reaction at 80 °C (Fig. 3a and Fig. S1a). The shell is smooth and homogeneous, and the cavity of the composite hollow colloid is clearly discerned from the TEM image. SnO_2 grew dominantly in the gel layer; no particles formed in either the dispersed phase or inside the cavity, confirming that the gel layer could favorably induce growth of SnO_2. The SnO_2 content is 37.4 wt.%, measured by TGA. The tetragonal phase of SnO_2 was confirmed by the X-ray diffraction (XRD) result (curve a of Fig. S2a, indexed at JCPDS no. 41-1445). The HR-TEM image (Fig. 3b) shows the {110}-lattice spacing of 0.335 nm. The SnO_2 nanocrystals are about 10 nm, which is consistent with the estimated result from XRD. The

composite hollow colloids were treated in air at 450 °C for 2 h to remove the polymer template. Consequently, SnO_2 hollow colloids were obtained with further SnO_2 crystallization. Osmotic pressure caused a slight perforation of the SnO_2 shell (Fig. S1b). The diffraction peaks in the XRD spectra remain in the same positions but became stronger and sharper, implying that thermal treatment facilitates further growth of the nanocrystals (curve b of Fig. S2a). BET surface areas of the composite hollow colloids before and after being calcined are 27.1 and 53.8 m^2/g, respectively. From the TEM image (Fig. 3c), it is found that the pores of the SnO_2 shell are mainly originated from the interstitial voids among the nanocrystals.

The similar procedure was employed to synthesize $In(OH)_3$/S2 composite hollow colloids. The shell is composed of cubic nanoparticles about 20 nm in diameter (Figs. 3d and S1c). The inorganic content is 32.2 wt.%. $In(OH)_3$ is in the cubic crystalline phase, which is confirmed by XRD (curve a, in Fig. S2b), HR-TEM ({200}-lattice spacing of 0.394 nm, Fig. 3e), and inset SAED results. In_2O_3 hollow colloids were formed after the as-prepared $In(OH)_3$/S2 composite colloids were calcined in air at 450 °C. The colloids become greatly shrunk (Fig. 3f). The crystallite remains in the cubic phase (curve a in Fig. 4; Fig. 3g indicating {222}-lattice spacing of 0.291 nm and inset SAED). After In_2O_3 was doped with Sn with an atomic content lower than 8 at.%, ITO hollow colloids were obtained by calcination of the as-prepared In–Sn hydroxide/S2 composite hollow colloids in air at 450 °C (Fig. 3h). The as-prepared In–Sn hydroxide/S2 colloid has the same crystalline phase as $In(OH)_3$, as certified from XRD spectra (curves a and b of Fig. S2b). The coexistence of In and Sn in ITO colloids was confirmed by EDX analysis (not shown here). The crystalline phase remains similar to In_2O_3 (curves a and b in Fig. 4). An excessive Sn-doped element at rates such as 16 at.% would result in phase separation of SnO_2 from ITO at high temperature, and the characteristic diffraction peaks corresponding to SnO_2 appear (curve c, Fig. 4).
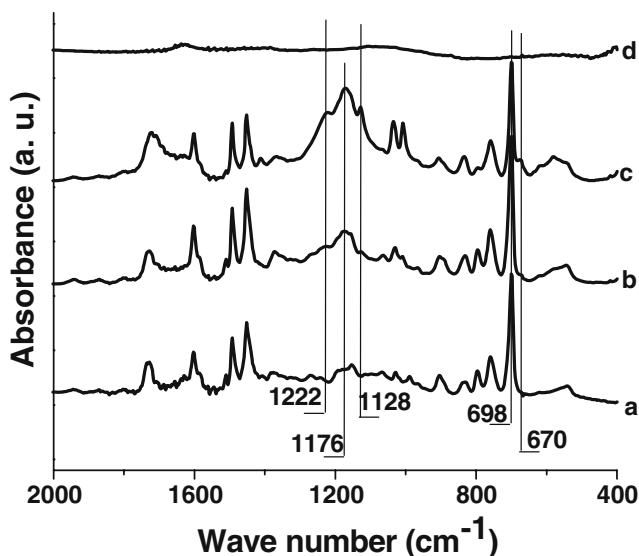
Fig. 2 FT-IR spectra of three representative polymer hollow colloids: **a** cross-linked PS hollow colloid; **b, c** sulfonated PS gel sphere S1 and S2 after the cross-linked PS colloid being sulfonated for 1 and 3 h, respectively; **d** carbon hollow colloid derived by carbonization of S2
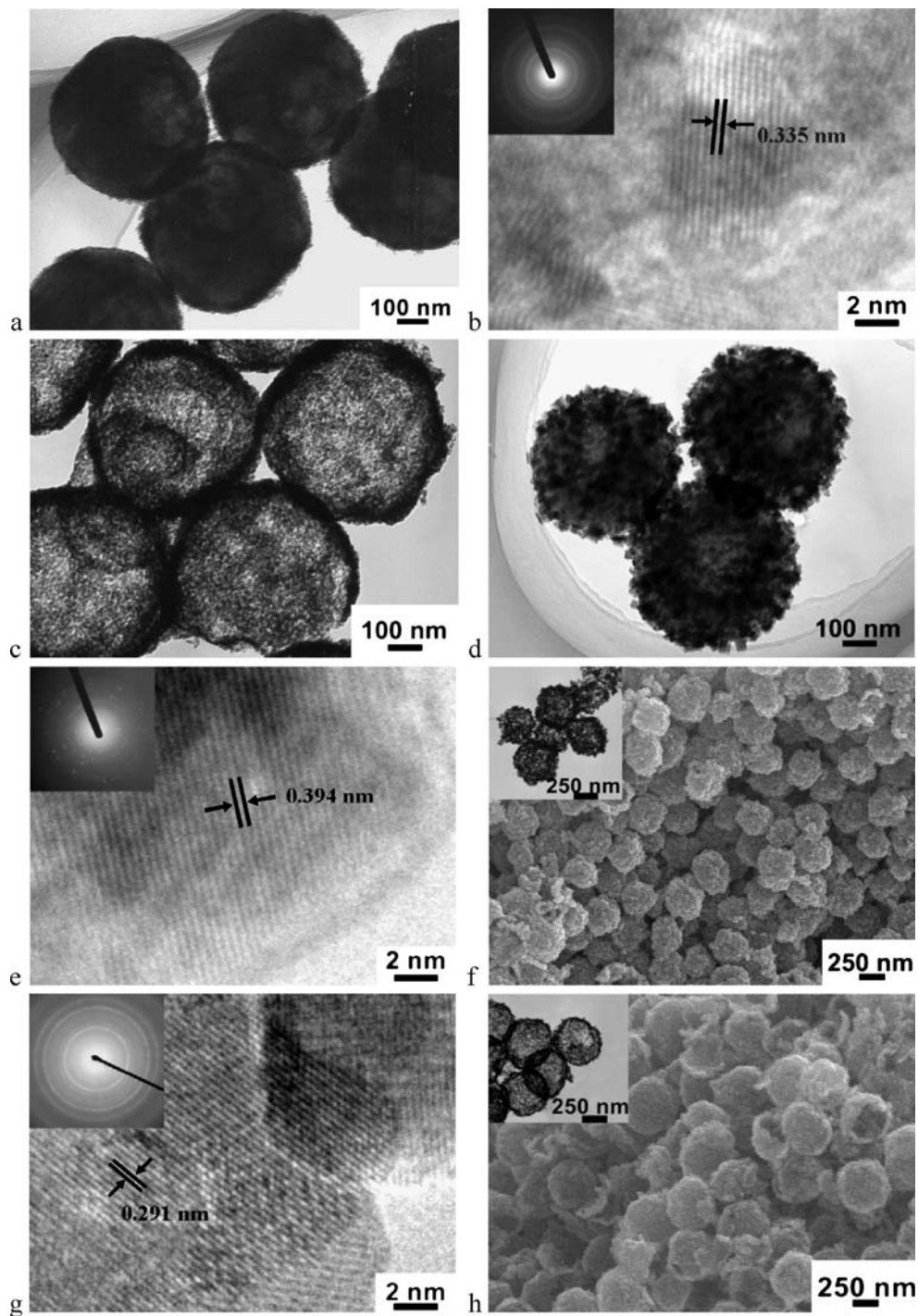
Fig. 3 **a** TEM image of SnO_2/S2 composite hollow colloids; **b** HR-TEM image of SnO_2 and *inset* SAED; **c** TEM image of SnO_2 hollow colloids after the as-prepared SnO_2/S2 being calcined at 450 °C in air; **d** TEM image of $In(OH)_3$/S2 composite hollow colloids; **e** HR-TEM image of a typical particle of $In(OH)_3$ and SAED (*inset*); **f** SEM and

TEM (*inset*) images of In_2O_3 hollow colloids prepared after $In(OH)_3$/S2 composite hollow colloids being calcined at 450 °C in air; **g** HR-TEM image of In_2O_3 and SAED (*inset*); **h** SEM and TEM (*inset*) images of ITO composite hollow colloids

The oxide/carbon composite hollow colloids

The sulfonated cross-linked PS could be carbonized by calcination at high temperature in inertia atmosphere [25, 26]. In our case, the sulfonated cross-linked PS hollow

colloids could be transformed into carbon by one step. From Fig. 5a and b, the carbon hollow colloids shrank but with the spherical shape well preserved. The prepared carbon hollow colloids are amorphous according to XRD [26] (curve a in Fig. 6) and Raman spectra in which two
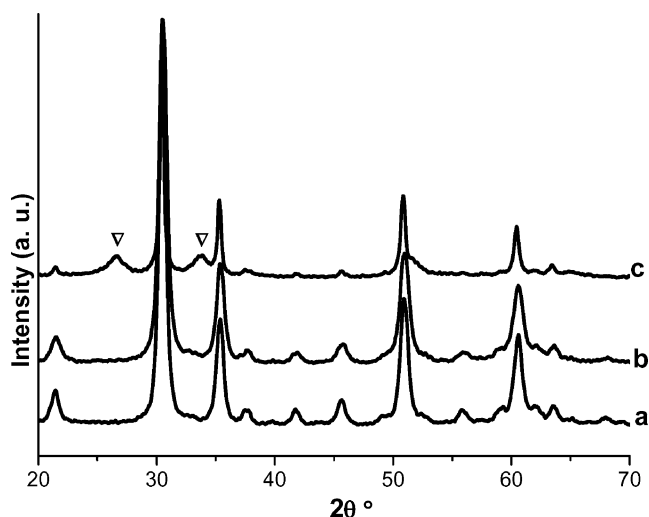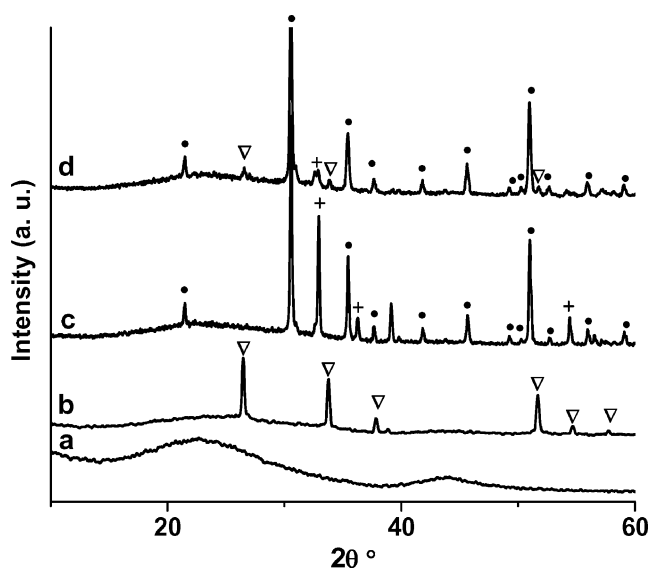
Fig. 4 XRD spectra of In–Sn oxide hollow colloids with 0, 8, and 16 at.% Sn doped corresponding to curves *a*, *b*, and *c*, respectively. *Reversed triangle*, SnO_2 (JCPDS no. 41-1445). Other diffractive peaks are attributed to In_2O_3 (JCPDS no. 71-2194)

broad bands at 1,320 and 1,590 cm^{-1} appear (not shown) [27]. Similarly, the oxide/carbon composite hollow colloids were directly derived by carbonization of the inorganic precursor/S2 composite hollow colloids. As an example, SnO_2/S2 composite hollow colloids were carbonized in nitrogen at 800 °C for 2 h (Fig. 5c and d). TEM (Fig. 5d) shows some large particles formed and isolated from the carbon surface. The narrow XRD diffraction peaks of SnO_2/carbon composite hollow colloids (curve b of Fig. 6) indicate that the crystalline SnO_2 size greatly increases. In $(OH)_3$/S2 composite colloids were carbonized the same way. The two crystalline phases of In_2O_3 and metal In are detected by XRD (curve c of Fig. 6). As shown in SEM and TEM images (Fig. 5e and f), the composite colloids are distorted, and some large cubes are scattered on the shells. After In_2O_3 was first transformed by decomposition of In $(OH)_3$ and grew into big particles, In_2O_3 particles could be further deoxidized by carbon into metal In at high

Fig. 5 a, b SEM and TEM images of carbon hollow colloids after S2 being treated at 800 °C in nitrogen; **c, d** SEM and TEM images of SnO_2/carbon composite hollow colloids; **e, f** SEM and TEM images of In_2O_3/In/carbon composite hollow colloids
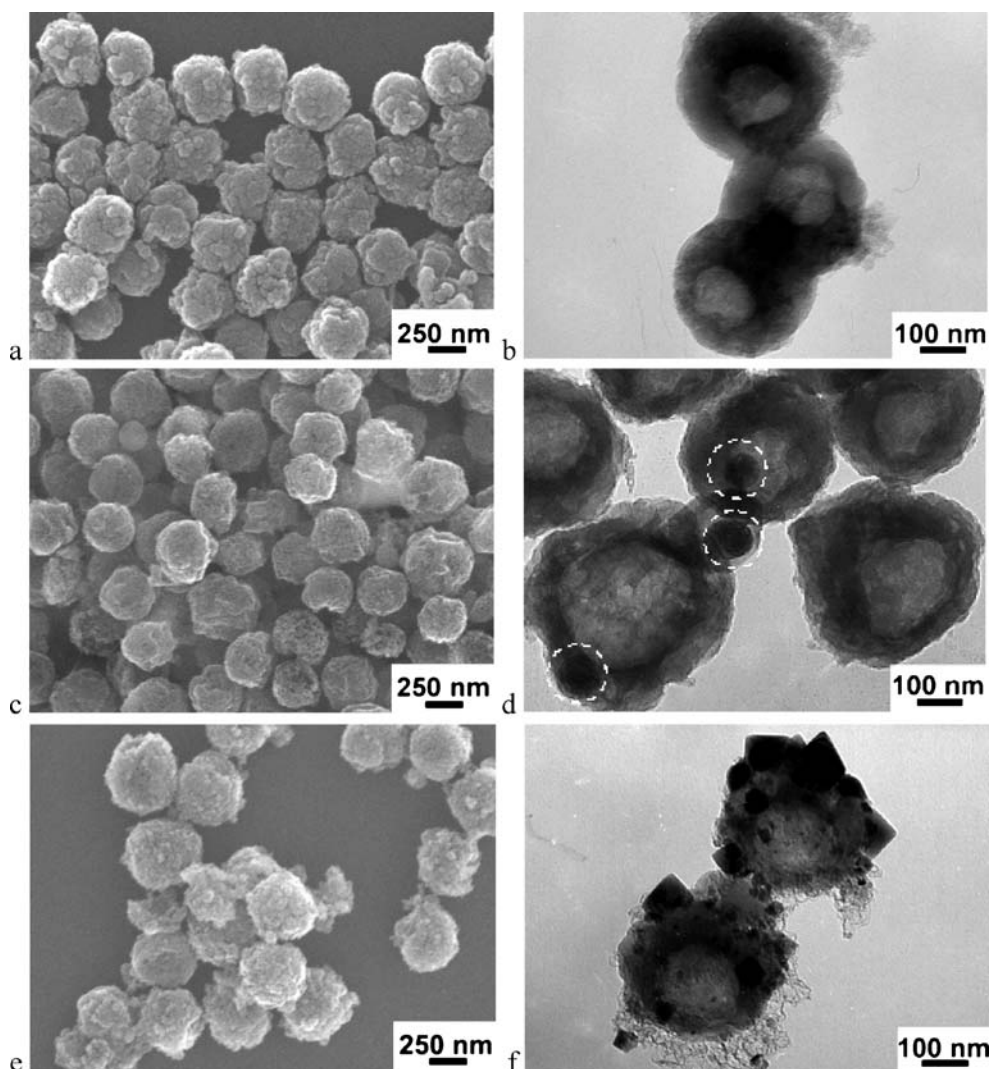
Fig. 6 XRD spectra of carbon and the carbon composite hollow colloids. **a** Carbon hollow colloids; **b** SnO_2/carbon composite hollow colloids; **c** In_2O_3/In/carbon composite hollow colloids; **d** ITO/In/SnO_2 carbon composite hollow colloids derived from 8 at.% Sn doped In–Sn hydroxide/S2. *Filled circles*, In_2O_3 (JCPDS no. 71-2194), *plus symbol*, In (JCPDS no. 85-1409), *reversed triangle*, SnO_2 (JCPDS no. 41-1445)

temperature. The oxide/carbon composite hollow colloids have a high BET surface area of ~500 m^2/g and nanosized pores (Fig. 7). In(OH)$_3$/S2 composite hollow colloids Sn doped at 8 at.% were carbonized the same way. There exists

a trace of SnO_2 separated from the ITO (curve d of Fig. 6) verified from XRD. The sample is therefore composed of ITO and a trace metal In and SnO_2 because of phase separation. The morphology of the carbonized sample is similar to that of the In_2O_3/In/carbon one.

Conclusion

The hollow colloids of the metal oxide/polymer and the derived carbon composites have been template synthesized. The gel layer of sulfonated PS hollow colloids can favorably induce adsorption of target precursors. The SnO_2, In_2O_3, and ITO hollow colloids are obtained via calcination in air to remove polymers. On the other hand, the sulfonated cross-linked PS hollow colloids can be directly carbonized into carbon. Therefore, the SnO_2, In_2O_3/In, and ITO/In/SnO_2 carbon composite hollow colloids are further derived by cabonization of the metal oxide/polymer composite colloids in nitrogen. The carbonization process leads to In_2O_3 reduction into metal In and separation of SnO_2 from the ITO structure when Sn-doped amount exceeds 8 at.%. The semiconductor/polymer and their corresponding carbon composite hollow colloids are promising as catalysts, sensors, and electrode materials.

Fig. 7 Nitrogen adsorption/desorption isotherms of the In_2O_3/In/carbon composite colloids and *inset* the corresponding pore size distribution calculated from the desorption branch of N_2 isotherm
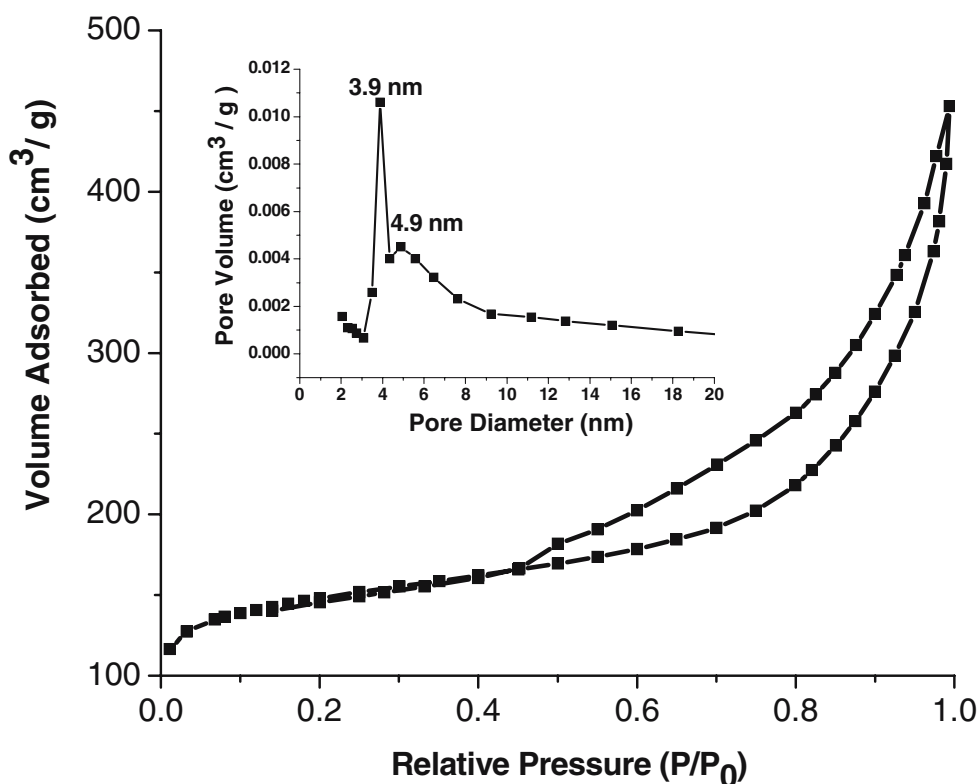
References

1. Caruso F, Caruso RA, Möhwald H (1998) Science 282:1111–1114
2. Caruso F (2001) Adv Mater 13:11–22 (and references therein)
3. Zhong ZY, Yin YD, Gates B, Xia YN (2000) Adv Mater 12:206–209
4. Zhu JJ, Lu ZH, Aruna ST, Aurbach D, Gedanken A (2000) Chem Mater 12:2557–2566
5. Jiang LH, Sun GQ, Zhou ZH, Sun SG, Wang Q, Yan SY, Li HQ, Tian J, Guo JS, Zhou B, Xin Q (2005) J Phys Chem B 109:8774–8778
6. Wang YL, Jiang XC, Xia YN (2003) J Am Chem Soc 125:16176–16177
7. Emons TT, Li JQ, Nazar LF (2002) J Am Chem Soc 124:8516–8517
8. Alam MJ, Cameron DC (2000) Thin Solid Films 377–378:455–459
9. Djaoued Y, Phong VH, Badilescu S, Ashrit PV, Girouard FE, Truong VV (1997) Thin Solid Films 293:108–112
10. Mattox DM (1991) Thin Solid Films 204:25–32
11. Bellingham JR, Mackenize AP, Philips WA (1991) Appl Phys Lett 58:2506–2508
12. Kim SM, Seo KH, Lee JH, Kim JJ, Lee HY, Lee JS (2006) J Eur Ceram Soc 26:73–80
13. Patra CR, Gedanken A (2004) New J Chem 28:1060–1065
14. Murali A, Barve A, Leppert VJ, Risbud SH, Kennedy LM, Lee HWH (2001) Nano Lett 1:287–289
15. Yu DB, Wang DB, Yu WC, Qian YT (2003) Mater Lett 58:84–87
16. Peng XS, Meng GW, Wang XF, Wang YW (2002) Chem Mater 14:4490–4493
17. Li BX, Xie Y, Jing M, Rong GX, Tang YC, Zhang GZ (2006) Langmuir 22:9380–9385
18. Zhang D, Sun L, Xu G, Yan C (2006) Phys Chem Chem Phys 8:4874–4880
19. Woon SB, Sohn K, Kim JY, Shin CH, Yu JS, Hyeon T (2002) Adv Mater 14:19–21
20. Kim M, Sohn K, Na HB, Hyeon T (2002) Nano Lett 2:1383–1387
21. Fan J, Wang T, Yu CZ, Tu B, Jiang ZY, Zhao DY (2004) Adv Mater 16:1432–1436
22. Wang Y, Zeng HC, Lee JY (2006) Adv Mater 18:645–649
23. Ding SJ, Zhang CL, Yang M, Qu XZ, Lu YF, Yang ZZ (2006) Polymer 47:8360–8366
24. Yang M, Ma J, Zhang CL, Yang ZZ, Lu YF (2005) Angew Chem Int Ed 44:6727–6730
25. Yoon SB, Kim JY, Yu JS (2001) Chem Commun 559–560
26. Nakagawa H, Watanabe K, Harada Y, Miura K (1999) Carbon 37:1455–1461
27. Tang C, Qi K, Wooley KL, Matyjaszewski K, Kowalewski T (2004) Angew Chem Int Ed 43:2783–2787